

Field enhancement at metallic interfaces due to quantum confinement

Z. Fatih Öztürk,^{a,b} Sanshui Xiao,^a Min Yan,^{a,c} Martijn Wubs,^a
Antti-Pekka Jauho,^{d,e} and N. Asger Mortensen^a

^a Department of Photonics Engineering, Technical University of
Denmark, DK-2800 Kongens Lyngby, Denmark

^b Istanbul Technical University, Istanbul, Turkey

^c Laboratory of Photonics and Microwave Engineering, Royal Institute of
Technology, Sweden

^d Department of Applied Physics, Aalto University, Finland

^e Department of Micro and Nanotechnology, Technical University of
Denmark, DK-2800 Kongens Lyngby, Denmark

Abstract. We point out an apparently overlooked consequence of the boundary conditions obeyed by the electric displacement vector at air-metal interfaces: the continuity of the normal component combined with the quantum mechanical penetration of the electron gas in the air implies the existence of a surface on which the dielectric function vanishes. This, in turn, leads to an enhancement of the normal component of the total electric field. We study this effect for a planar metal surface, with the inhomogeneous electron density accounted for by a Jellium model. We also illustrate the effect for equilateral triangular nanoislands via numerical solutions of the appropriate Maxwell equations, and show that the field enhancement is several orders of magnitude larger than what the conventional theory predicts.

Keywords: Nanoplasmonics, field enhancement, Friedel oscillations, zero-epsilon phenomena

1 INTRODUCTION

Electromagnetic field enhancement in nanoplasmonic structures plays an important role in a number of applications such as nano antennas [1, 2], single-photon emitters [3], and surface-enhanced spectroscopy techniques in general [4], including surface-enhanced Raman spectroscopy (SERS) [5]. Field localization is the key to understanding and further enhancing the resolution of SERS, and the use of highly engineered surface plasmonic structures has been envisioned [6, 7]. Strong field enhancement has so far been inherently connected to singularities [8].

It is commonplace to study the plasmonic response using Maxwell's equations with the bulk dielectric function of the metal, with an abrupt change at the air-metal interface [9]. Though clearly neglecting surface and confinement effects for the electrons in the metal, this is a celebrated approximation which predicts the existence of surface plasmons forming the heart of nanoplasmonics. However, when samples involve true nano-scale feature-sizes, the validity of this approximation is challenged and new phenomena, such as non-local response and spatial dispersion [10–17] and inhomogeneous electron densities due to quantum confinement [18, 19] are expected to play an important role.

Send correspondence to N.A.M.: asger@mailaps.org

In nanoscale metallic structures the electrons are subject to quantum confinement, which leads to a number of spectacular effects, such as the quantized conductance of atomic quantum-point contacts [20], Friedel oscillations and confinement of electrons to quantum corrals on noble metal surfaces [21], and a size-dependent structure of nanocrystals [22]. Light emission from STM has been used to reveal plasmonic properties of electrons confined to triangular islands on surfaces of noble metals [23]. All these studies clearly show that, at least at low temperatures, quantum confinement plays an important role leading to inhomogeneous electron densities at interfaces that differ from the piecewise constant bulk values.

2 FROM BULK APPROXIMATION TO A LOCAL DENSITY APPROXIMATION

The qualitative optical consequences of an inhomogeneous electron density can be explored within Lindhard’s “*local density approximation*” for the dielectric function [24, 25]

$$\epsilon(\mathbf{r}, \omega) = 1 - \frac{\omega_p^2}{\omega(\omega + i\gamma)} \Pi(\mathbf{r}) \quad (1)$$

where $\Pi(\mathbf{r}) = n(\mathbf{r})/n_0$ accounts for the density variations relative to the bulk density of electrons $n_0 = m\omega_p^2/e^2$, with ω_p being the bulk plasma frequency. To mimic the Ohmic damping we have included a damping rate γ and in the optical regime $\gamma \ll \omega$ [26]. While several studies have considered the consequences of local density variations for the surface-plasmon dispersion relation, the overall effects have been reported to be minor and for planar surfaces the surface-plasmon resonance at $\omega = \omega_p/\sqrt{2}$ appears unaffected by the detailed density profile at the metal-air surface [27]. However, it remains an open question to which extent the detailed field distribution will be affected by a smoothly varying electron density in contrast to the discontinuous drop in the electron density assumed by the bulk approximation.

Zero-index phenomena in metamaterials are receiving increasing attention [28–33], and the recent results by Litchinitser *et al.* [34] show that for a metamaterial with the effective constitutive coefficients varying linearly, $\epsilon(z) \propto z$ and $\mu(z) \propto z$, a pronounced field enhancement will occur at $z = 0$ where $\epsilon = \mu = 0$. In this paper we show that plasmonic structures employing Nature’s own metals may support large field enhancement at the zero- ϵ surface appearing in the vicinity of the air-metal interface, where the real part of the polarization of the dilute electron gas will exactly balance the polarization of the vacuum background. As shown below, the particular position of the zero- ϵ surface depends on the frequency ω of the incident radiation, and may be either in air or in the metal, depending on the local geometry.

3 PHENOMENOLOGY OF FIELD ENHANCEMENT

The basic mechanism behind the field enhancement can be understood from the continuity condition for the electrical displacement field, which stipulates that $\mathbf{n} \cdot \mathbf{D} = \epsilon(\mathbf{n} \cdot \mathbf{E})$ be continuous (here \mathbf{n} is the normal vector of a surface element). At the zero- ϵ surface the normal component $E_\perp = \mathbf{n} \cdot \mathbf{E}$ thus has to diverge to keep the product ϵE_\perp finite.

From Eq. (1) it follows that in the regions where $\text{Re}(\epsilon)$ vanishes, there will still be a small, but finite imaginary part: $\text{Im}(\epsilon)_{\text{Re}(\epsilon)=0} = \gamma/\omega$. For an electrical field \mathbf{E}_0 incident at an angle θ we thus expect that the normal component $\mathbf{n} \cdot \mathbf{E}_0 = E_0 \sin \theta$ is enhanced by a factor proportional to $1/\gamma$ on the zero- ϵ surface. The intensity enhancement can then be estimated as

$$|\mathbf{E}|^2/|\mathbf{E}_0|^2 \propto \sin^2 \theta / \gamma^2 \quad (2)$$

We emphasize that this mechanism of field-enhancement is generic and robust as it only depends on the assumed continuous negative-to-positive variation of the dielectric function at the metal-air interface, in combination with a Maxwell boundary condition [35], rather than on the details of the excitation of strongly localized surface-plasmon resonances with pronounced sample-to-sample fluctuations.

4 EXAMPLE 1: JELLIUM MODEL FOR THE METAL SURFACE

The low-temperature density profile for Jellium is a function of r_s/a_0 only, with the radius of the free-electron sphere $r_s = (3/4\pi n_0)^{1/3}$ and $a_0 = \hbar^2/me^2$ being the Bohr radius. The position-dependent electron density may be obtained self-consistently with the aid of density-functional theory [36], thus taking into account both exchange and correlation effects in the inhomogeneous electron gas. In Ref. [36], results are tabulated for a range of values of r_s/a_0 . The resulting density $n(z)$ is shown in Fig. 1(a) for $r_s/a_0 = 2$, a typical value for gold or silver. As seen, $\Pi(z) = n(z)/n_0$ varies continuously on the length scale of the Fermi wavelength rather than exhibiting a discontinuous drop at the surface of the metal ($z = 0$). In the metal ($z > 0$), there are Friedel oscillations near the surface, while for $z < 0$ the decay of the density is caused by the finite value of the work function W , which allows electron wave functions to penetrate into the classically forbidden region. According to Eq. (1), the dielectric function will inherit the Friedel oscillations in the metal, as well as approach the value in vacuum outside the metal surface. As a consequence, the dielectric function passes through zero just outside the metal surface [green line in Fig. 1(a)]. Similar spatial variations of the dielectric function have been reported in more elaborate studies of e.g. semiconductor quantum dots [37] and recently also in doped semiconductors [38].

In the case of $\lambda = 2\pi c/\omega = 633$ nm the zero- ϵ surface appears at a distance of 0.25 nm from the surface ($z = 0$). Fig. 1(b) illustrates the field enhancement in the case of a plane wave incident at an angle of $\theta = 60^\circ$. The numerical results were obtained by solving the wave equation

$$\nabla \times \nabla \times \mathbf{E}(\mathbf{r}) = \epsilon(\mathbf{r}, \omega) \frac{\omega^2}{c^2} \mathbf{E}(\mathbf{r}) \quad (3)$$

with the aid of a finite-element method employing an adaptive mesh algorithm (Comsol Multi-Physics). A comparison with $\epsilon(z)$ in Fig. 1 (a) shows that the field enhancement indeed occurs at the point where $\epsilon = 0$. We emphasize that this phenomenon has no counterpart within the classical bulk approximation of the dielectric function. For a realistic value of the damping ($\gamma = 1 \times 10^{14}$ rad/s) the intensity may be enhanced by more than 3 orders of magnitude, which suggests that in a SERS experiment the Raman signal could be enhanced by 6 orders of magnitude [39] without the need for any geometry-induced localized resonances. To further test the predictions of Eq. (2) we have explored the dependence on the angle of incidence as well as the particular value of the plasmon damping. Fig. 2 (a) illustrates how the peak height depends on damping. The enhancement is limited by the plasmonic damping with the slope of the dashed lines being in full accordance with the power (-2) of γ in Eq. (2). Panel (b) illustrates the angle dependence with the dashed line showing the $\sin^2 \theta$ dependence of Eq. (2), indicating a pronounced enhancement for oblique incidence.

5 EXAMPLE 2: A METALLIC NANOSTRUCTURE

We next explore the field enhancement in the presence of strong confinement of electrons in metallic nanostructures. Here we limit ourselves to a model of non-interacting electrons in wire geometries with nanoscale cross sections Ω so that the problem effectively is two-dimensional. The energy states of the electron system are then given by $\mathcal{E}(\kappa) = \frac{\hbar^2}{2m}\kappa^2 + \mathcal{E}_\nu$ with the transverse energy components being quantized and governed by a two-dimensional Schrödinger equation

$$\left[-\frac{\hbar^2}{2m} \nabla_{xy}^2 + V(x, y) \right] \psi_\nu(x, y) = \mathcal{E}_\nu \psi_\nu(x, y). \quad (4)$$

For the confinement potential V we adjust the height in accordance with the work function of the metal $W = V_0 - \mu$, where μ is the chemical potential. In equilibrium the states are populated

according to the Fermi–Dirac distribution function and we find

$$\Pi(x, y) \equiv \frac{n(x, y)}{n_0} = \frac{\sum_{\nu} P\left(\frac{\epsilon_{\nu} - \mu}{k_B T}\right) A |\psi_{\nu}(x, y)|^2}{\sum_{\nu} P\left(\frac{\epsilon_{\nu} - \mu}{k_B T}\right)} \quad (5)$$

where $A = \int_{\Omega} dx dy$ is area and $P(x) = \text{Li}_{1/2}[-\exp(-x)]$ with $\text{Li}_n(x)$ being Jonqui ere’s polylogarithm function. Equilateral triangular nano islands have been the subject of numerous investigations [40, 41] and in Fig. 3 we consider field enhancement in such a structure. Fig. 3(a) shows results within the bulk approximation, where an artificial rounding of the corners has been added to circumvent the effect of an otherwise divergent electrical field [7]. Clearly, field enhancement is modest since no pronounced surface plasmon resonances are excited. Fig. 3(b) on the other hand is based on the spatially continuously varying dielectric function of Eqs. (1) and (5) and shows a pronounced field enhancement along the zero- ϵ surface. We also note that while the geometry has arbitrarily sharp corners, the electron density and dielectric function themselves are still smooth, showing that quantum confinement provides a built-in smoothing even in the presence of sharp geometrical features. Fig. 4(a) and (b) show in more detail the field enhancement along the lines indicated in Fig. 3(b). For the results in Fig. 4(b), the peak height clearly matches the one-dimensional results in panel (b) of Fig. 2 for an incident angle of $\theta = 30^\circ$. Similarly, the result within the bulk approximation resembles typical results, see e.g. Ref. [35], i.e. the field enhancement is more modest. In Fig. 4(a), the incident wave propagates almost parallel to the zero- ϵ surface ($\theta \sim 90^\circ$), thus causing a peak that is even higher at the two right-most corners of the triangle. On the other hand, at the left-most corner the wave has normal impact on the zero- ϵ surface ($\theta = 0^\circ$) so that no pronounced field enhancement is observed. It is interesting to note that the enhancement may occur either outside [as in Fig. 1(b)] or inside [as in Fig. 3(b)] the metal, depending on the local geometry and the frequency relative to the plasma frequency.

6 CONCLUSIONS

We predict that a large non-resonant field enhancement may occur at zero-epsilon surfaces near the air-metal interface. Theoretically, the enhancement occurs in a wide class of models where the discontinuous jump of the dielectric function of the usual bulk description of at an air-metal interface is replaced by a continuous function $\epsilon(\mathbf{r}, \omega)$ that has the bulk values as limiting values away from the interface. We discussed two microscopic models for such a continuous variation at the interface. The predicted field enhancement has therefore no counterpart in the classical bulk treatment of plasmonic field enhancement, though it is intimately related to the familiar boundary condition for the electrical displacement field. In particular, for light impinging on an interface we discussed the dependence of the field enhancement on the angle of incoming light and on the damping in the metal. Furthermore, the enhancement constitutes another mechanism for the enhancement of Raman signals at metal interfaces (SERS).

Interestingly, Feigenbaum *et al.* have recently reported their experimental observation of zero-index driven field enhancement at the surface of conducting oxides (i.e. with lower electron density compared to good metals) [38]. We emphasize that the decay of the electron density into vacuum (or more generally into a dielectric) could have important implications also for nano-gap structures (such as the gap formed between the corners of two nearby triangles [40]), where quantum tunneling of electrons will introduce a small but finite electron density inside the gap, thus also modifying the local dielectric function and the ability to support short-circuiting currents [19].

Acknowledgments

We thank Peter Nordlander, Natalia M. Litchinitser, and Vladimir M. Shalaev for useful discussions. This work is financially supported by the Danish Council for Strategic Research through the Strategic Program for Young Researcher (grant no: 2117-05-0037), the Danish Research Council for Technology and Production Sciences (grants no: 274-07-0080 & 274-07-0379), as well as the FiDiPro program of the Finnish Academy.

References

- [1] P. Mühlischlegel, H.-J. Eisler, O. J. F. Martin, B. Hecht, and D. W. Pohl, “Resonant optical antennas,” *Science* **308**(5728), 1607 – 1609 (2005).
- [2] L. Novotny, “Effective wavelength scaling for optical antennas,” *Phys. Rev. Lett.* **98**(26), 266802 (2007).
- [3] D. E. Chang, A. S. Sørensen, E. A. Demler, and M. D. Lukin, “A single-photon transistor using nanoscale surface plasmons,” *Nat. Phys.* **3**(11), 807 – 812 (2007).
- [4] M. Moskovits, “Surface-enhanced spectroscopy,” *Rev. Mod. Phys.* **57**(3), 783 – 826 (1985).
- [5] M. Fleischmann, P. J. Hendra, and A. J. McQuillan, “Raman-spectra of pyridine adsorbed at a silver electrode,” *Chem. Phys. Lett.* **26**(2), 163 – 166 (1974).
- [6] S. Lal, S. Link, and N. J. Halas, “Nano-optics from sensing to waveguiding,” *Nat. Phot.* **1**(11), 641 – 648 (2007).
- [7] S. Xiao, N. A. Mortensen, and A.-P. Jauho, “Nanostructure design for surface-enhanced Raman spectroscopy-prospects and limits,” *J. Europ. Opt. Soc. Rap. Public.* **3**, 08022 (2008).
- [8] Y. Luo, J. B. Pendry, and A. Aubry, “Surface plasmons and singularities,” *Nano Lett.* **10**(10), 4186 – 4191 (2010).
- [9] S. A. Maier, *Plasmonics: Fundamentals and Applications*, Springer, New York (2007).
- [10] J. Lindhard, “On the properties of a gas of charged particles,” *Mat. Fys. Medd. Dan. Vid. Selsk.* **28**(8), 1 – 57 (1954).
- [11] A. D. Boardman, B. V. Paranjape, and Y. O. Nakamura, “Surface plasmon-polaritons in a spatially dispersive inhomogeneous medium,” *Phys. Stat. Solid. (b)* **75**(1), 347 – 359 (1976).
- [12] B. B. Dasgupta and R. Fuchs, “Polarizability of a small sphere including nonlocal effects,” *Phys. Rev. B* **24**(2), 554–561 (1981).
- [13] R. Chang and P. T. Leung, “Nonlocal effects on optical and molecular interactions with metallic nanoshells,” *Phys. Rev. B* **73**(12), 125438 (2006).
- [14] F. J. García de Abajo, “Nonlocal effects in the plasmons of strongly interacting nanoparticles, dimers, and waveguides,” *J. Phys. Chem C* **112**(46), 17983–17987 (2008).
- [15] J. M. McMahon, S. K. Gray, and G. C. Schatz, “Nonlocal optical response of metal nanostructures with arbitrary shape,” *Phys. Rev. Lett.* **103**(9), 097403 (2009).
- [16] J. M. McMahon, S. K. Gray, and G. C. Schatz, “Calculating nonlocal optical properties of structures with arbitrary shape,” *Phys. Rev. B* **82**(3), 035423 (2010).
- [17] J. M. McMahon, S. K. Gray, and G. C. Schatz, “Optical properties of nanowire dimers with a spatially nonlocal dielectric function,” *Nano Lett.* **10**(9), 3473–3481 (2010).
- [18] J. Zuloaga, E. Prodan, and P. Nordlander, “Quantum description of the plasmon resonances of a nanoparticle dimer,” *Nano Lett.* **9**(2), 887 – 891 (2009).
- [19] O. Perez-Gonzalez, N. Zabala, A. G. Borisov, N. J. Halas, P. Nordlander, and J. Aizpurua, “Optical spectroscopy of conductive junctions in plasmonic cavities,” *Nano Lett.* **10**(8), 3090 – 3095 (2010).
- [20] A. I. Yanson, G. R. Bollinger, H. E. van den Brom, N. Agraït, and J. M. van Ruitenbeek, “Formation and manipulation of a metallic wire of single gold atoms,” *Nature* **395**(6704), 783 – 785 (1998).
- [21] M. F. Crommie, C. P. Lutz, and D. M. Eigler, “Confinement of electrons to quantum corrals on a metal surface,” *Science* **262**(5131), 218–220 (1993).
- [22] J. V. Lauritsen, J. Kibsgaard, S. Helveg, H. Topsøe, B. S. Clausen, E. Lægsgaard, and F. Besenbacher, “Size-dependent structure of MoS₂ nanocrystals,” *Nat. Nanotechnol.* **2**(1), 53 – 58 (2007).

- [23] G. Schull, M. Becker, and R. Berndt, “Imaging confined electrons with plasmonic light,” *Phys. Rev. Lett.* **101**(13), 136801 (2008).
- [24] J. Lindhard and M. Scharff, “Energy loss in matter by fast particles of low charge,” *Mat. Fys. Medd. Dan. Vid. Selsk.* **27**(15), 1 – 31 (1953).
- [25] H. Nitta, S. Shindo, and M. Kitagawa, “Classical theory of the dielectric function for an inhomogeneous electron gas,” *Surf. Sci.* **286**(3), 346 – 354 (1993).
- [26] Our qualitative conclusions do not change if a more sophisticated form for the dielectric function is adopted, such as the charge-conserving form due to N. D. Mermin, *Phys. Rev. B* **1**(5), 2362 (1970).
- [27] A. Boardman, B. Paranjape, and R. Teshima, “The effect of structure on surface plasmons,” *Surf. Sci.* **49**(1), 275 – 292 (1975).
- [28] N. García, E. V. Ponizovskaya, and J. Q. Xiao, “Zero permittivity materials: Band gaps at the visible,” *Appl. Phys. Lett.* **80**(7), 1120–1122 (2002).
- [29] M. Silveirinha and N. Engheta, “Tunneling of electromagnetic energy through subwavelength channels and bends using epsilon-near-zero materials,” *Phys. Rev. Lett.* **97**(15), 157403 (2006).
- [30] Q. Cheng, R. Liu, D. Huang, T. J. Cui, and D. R. Smith, “Circuit verification of tunneling effect in zero permittivity medium,” *Appl. Phys. Lett.* **91**(23), 234105 (2007).
- [31] R. Liu, Q. Cheng, T. Hand, J. J. Mock, T. J. Cui, S. A. Cummer, and D. R. Smith, “Experimental demonstration of electromagnetic tunneling through an epsilon-near-zero metamaterial at microwave frequencies,” *Phys. Rev. Lett.* **100**(2), 023903 (2008).
- [32] B. Edwards, A. Alù, M. E. Young, M. Silveirinha, and N. Engheta, “Experimental verification of epsilon-near-zero metamaterial coupling and energy squeezing using a microwave waveguide,” *Phys. Rev. Lett.* **100**(3), 033903 (2008).
- [33] R. J. Pollard, A. Murphy, W. R. Hendren, P. R. Evans, R. Atkinson, G. A. Wurtz, A. V. Zayats, and V. A. Podolskiy, “Optical nonlocalities and additional waves in epsilon-near-zero metamaterials,” *Phys. Rev. Lett.* **102**(12), 127405 (2009).
- [34] N. M. Litchinitser, A. I. Maimistov, I. R. Gabitov, R. Z. Sagdeev, and V. M. Shalaev, “Metamaterials: electromagnetic enhancement at zero-index transition,” *Opt. Lett.* **33**(20), 2350–2352 (2008).
- [35] T. Søndergaard and S. I. Bozhevolnyi, “Slow-plasmon resonant nanostructures: Scattering and field enhancements,” *Phys. Rev. B* **75**(7), 073402 (2007).
- [36] N. D. Lang and W. Kohn, “Theory of metal surfaces: Charge density and surface energy,” *Phys. Rev. B* **1**(12), 4555–4568 (1970).
- [37] X. Cartoixa and L. W. Wang, “Microscopic dielectric response functions in semiconductor quantum dots,” *Phys. Rev. Lett.* **94**(23), 236804 (2005).
- [38] E. Feigenbaum, K. Diest, and H. A. Atwater, “Unity-order index change in transparent conducting oxides at visible frequencies,” *Nano Lett.* **10**(6), 2111–2116 (2010).
- [39] F. J. García-Vidal and J. B. Pendry, “Collective theory for surface enhanced Raman scattering,” *Phys. Rev. Lett.* **77**(6), 1163 – 1166 (1996).
- [40] A. Sundaramurthy, P. J. Schuck, N. R. Conley, D. P. Fromm, G. S. Kino, and W. E. Moerner, “Toward nanometer-scale optical photolithography: Utilizing the near-field of bowtie optical nanoantennas,” *Nano Lett.* **6**(3), 355–360 (2006).
- [41] J. Nelayah, M. Kociak, O. Stéphan, F. J. García de Abajo, M. Tencé, L. Henrard, D. Taverna, I. Pastoriza-Santos, L. M. Liz-Marzán, and C. Colliex, “Mapping surface plasmons on a single metallic nanoparticle,” *Nat. Phys.* **3**(5), 348–353 (2007).

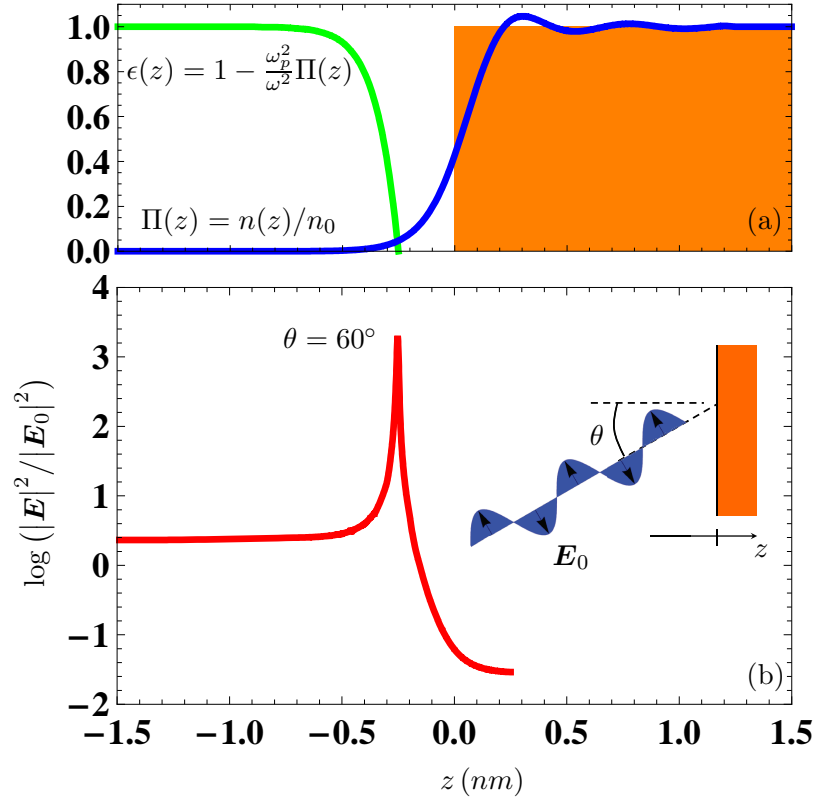


Fig. 1. (a) The blue line shows the position dependent electron density within the Jellium model ($r_s/a_0 = 2$). The green line shows the corresponding derived dielectric function. (b) The field enhancement for a plane wave incident on the surface at an angle of $\theta = 60^\circ$, for $\lambda = 633$ nm, $\omega_p = 1.37 \times 10^{16}$ rad/s, and $\gamma = 1.0 \times 10^{14}$ rad/s.

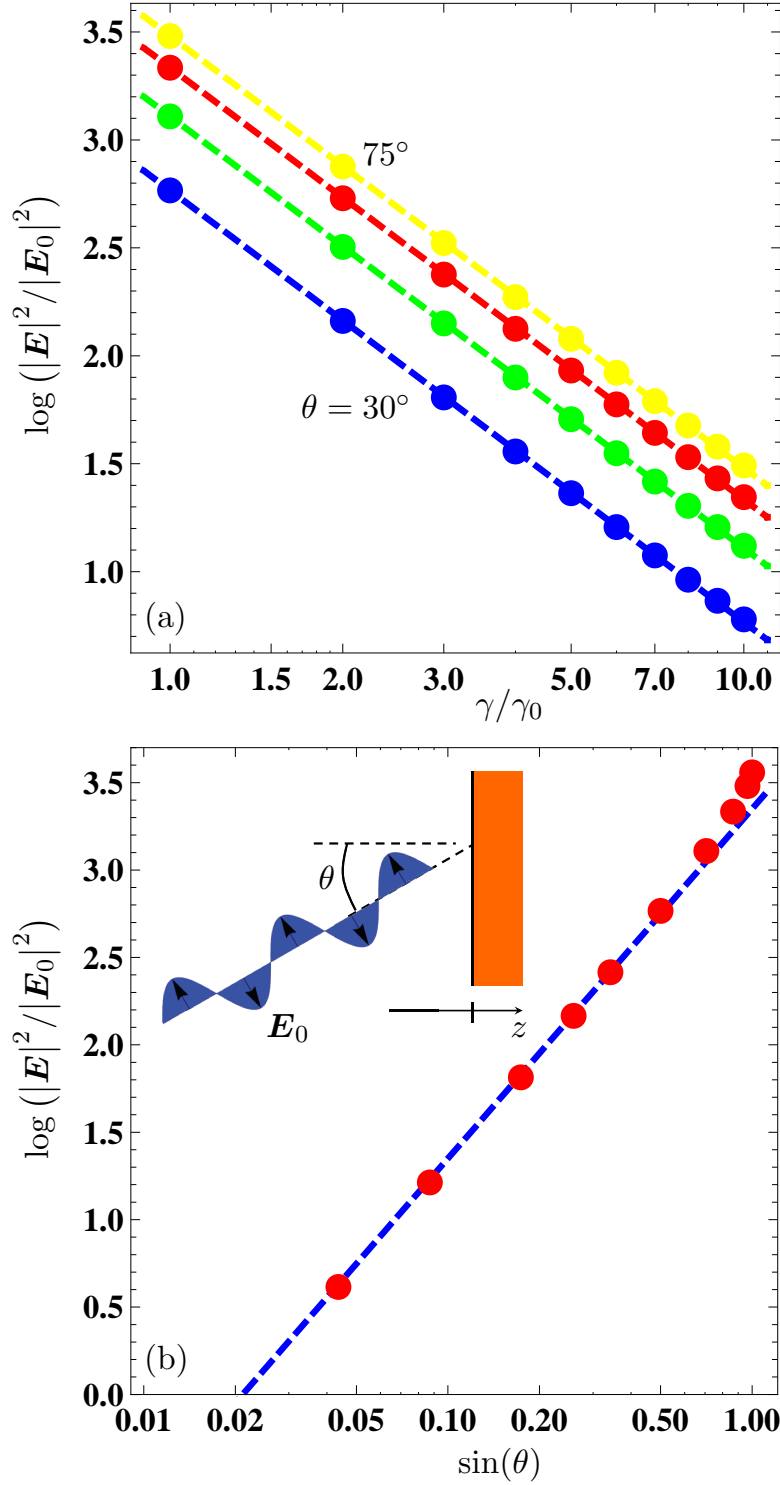


Fig. 2. (a) Maximal field enhancement as a function of damping for parameters of Fig. 1(b). The dashed lines indicate a γ^{-2} dependence. (b) The peak height as a function of incident angle for $\gamma = 1.0 \times 10^{14}$ rad/s. The dashed line indicates a $\sin^2 \theta$ dependence, Eq.(2).

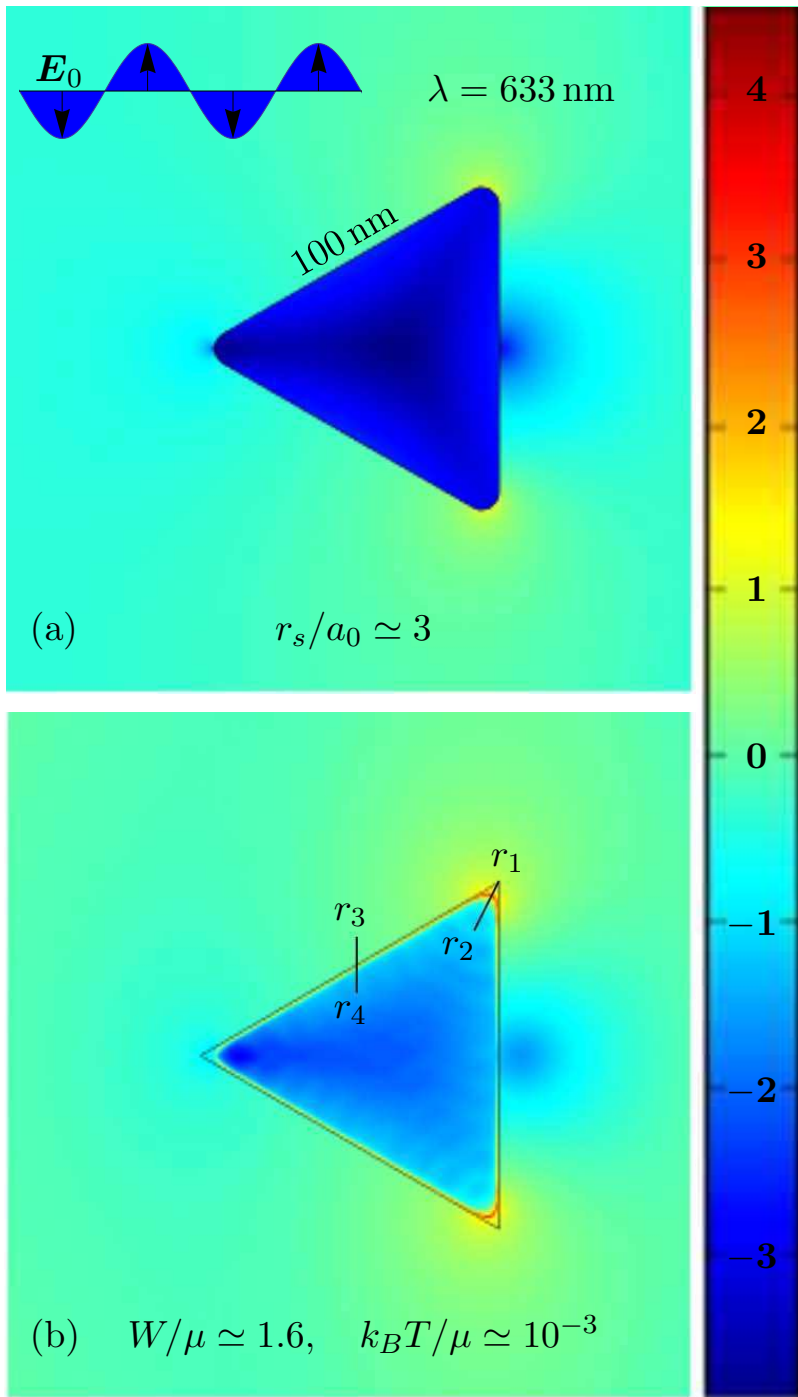


Fig. 3. (a) Intensity enhancement (log scale) for a wave incident from the left on a metallic equilateral triangle, computed with the bulk dielectric function, but with rounded corners (radius of 5 nm). (b) Field enhancement for the inhomogeneous density. Field profiles along the lines $r_1 \rightarrow r_2$ and $r_3 \rightarrow r_4$ are shown in Fig. 4.

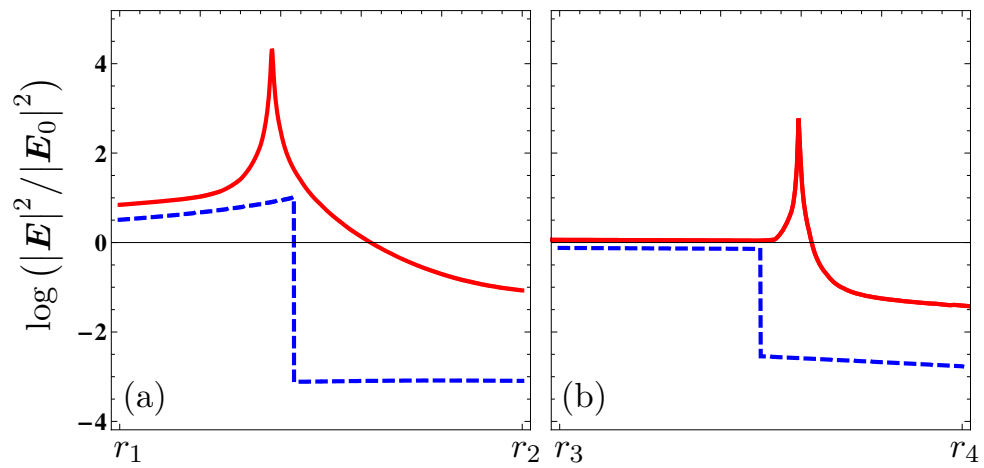


Fig. 4. Field enhancement along the lines defined in Fig. 3. (a) $r_1 \rightarrow r_2$. (b) $r_3 \rightarrow r_4$. Note that the integrated density is the same for the two structures in Fig. 3, thus causing slightly different densities and field suppression inside the metal structures (compare dashed and solid lines for the inhomogeneous and homogeneous cases, respectively).